J Them Anal Calorim (2013) 114:979–987
DOI 10.1007/s10973-013-3331-9

Treated and untreated foam core particleboards with intumescent veneer

Comparative analysis using a cone calorimeter

Mark A. Dietenberger · Ali Shalbafan · Johannes Welling · Charles Boardman

Received: 11 January 2013/ Accepted: 5 July 2013/Published online: 30 July 2013

Abstract The effectiveness of treatments for the surface layer of novel foam core particleboards was evaluated by means of Cone calorimeter tests. Foam core particleboards with variations of surface layer treatment, adhesives, and surface layer thicknesses under similar processing conditions were used to produce the test specimen for the Cone calorimeter tests. Ignitability, heat release rate profile, peak of heat release rate, total heat released, effective heat of combustion, mass loss rate, gaseous emissions, and specific extinction area were measured using the cone irradiance of 50 kW m^{-2}. Additional analysis of this data provided fuel composition information that could reveal the pyrolysis events of the composite boards. Thermocouples at various depths were used to provide further verification of pyrolysis events. The unprotected foam core panels generally had much higher heat release rates, somewhat higher heat of combustion and much higher smoke production due to the polymeric foam component of tested panels, whereas time to ignition and total heat release were not pronounced from the veneer treated boards. Adding the commercial fire retardant veneer to the face particleboard provided a dramatic improvement to the measured flammability properties. It worked sufficiently well with a 3 mm thick surface layer to improve the predicted flame spread rating of the foam core particleboards.

Keywords Foam core particleboard · Cone calorimeter · Sandwich · FRT veneer · Polystyrene foam

M. A. Dietenberger (✉) · C. Boardman
Forest Products Laboratory, USDA Forest Service, One Gifford Pinchot Drive, Madison, WI 53726-2398, USA
e-mail: mdietenberger@fs.fed.us

A. Shalbafan
Department of Wood Science, University of Hamburg 21031 Hamburg, Gemany

J. Welling
Institute of Wood Technology and Wood Biology, Thuenen-Institute (TI), 2103 Hamburg, Gemany

Introduction

A novel technology to produce lightweight, sandwich-type composites with particleboard facing and a foam core in one single production step has been developed [1]. This type of particleboard and foam core panel can be produced on standard particleboard production lines which can be adapted to the new technology with some modifications of the machines. The presence of the expandable polystyrene (EPS) for in situ foaming of the core material implies some restrictions in the production process. But also the fire safety of this type of innovative panel might become a crucial aspect when introducing these novel panels into the market. The cone calorimeter for evaluating flammability has gained very wide acceptance world-wide and has been considered to be especially useful for the development of new products [2, 3]. This ASTM E 1354-11a [4] test apparatus measures the relevant reaction-to-fire parameters that have good correlations to full-scale fire behavior. The ignition time, heat release rate, total heat released, heat of combustion, mass loss rate, combustion products, and specific extinction area are the main parameters measured and analyzed with ASTM 1354-11a. The need for a comprehensive investigation of fire performance of foam core sandwich panels is indicated by the limited studies available on similar thin foam core sandwich panels.

The first study in this project involved the cone calorimeter tests of samples exposed in the horizontal orientation with the conical radiant electric heater set at the irradiance 35 kW m^{-2}. By testing 19 mm thick panels with variations in surface layer thicknesses, core foam densities, and processing temperatures, it was found that the surface layers have an important impact on the fire behavior of sandwich structures [5]. In that study, the heat release rates (HRR) for the sandwich panels were much higher than for the conventional particleboard panel. Their flammability properties improved as the surface layer thicknesses increased from 3 to 5 mm. However, the levels of HRR were similar to some existing wood-based panels, and thus should have at least some market use on that basis.

It is interesting that the EPS foam has thermal properties that suggest a fire retardant solution. It is stated that the polystyrene foams start to soften and shrink from 100 °C and melt at even higher temperatures (around 250 °C). Upon further heating, ignitable decomposition gases are created at about 350 °C. Without a flame source, temperatures above 450–500 °C lead to the ignition of the decomposition products. When exposed to a small flame, the flame retarded polystyrene melts away from the ignition source without itself igniting and ignition might only be observed after longer flame exposures. If the contact with the external flame stops, further burning or smoldering might not be observed. In conjunction with other combustible substances, even flame retarded polystyrene foam can burn [6]. Thus to avoid this burning condition, the polystyrene can be kept below its decomposition temperatures via the insulation effects of either a thicker surface layer or the use of surface intumescent veneer or coating. The testing of the commercial intumescent surface layer with a high fire rating required the use of the more severe cone irradiance of 50 kW m^{-2}, which is associated with large fires and severe reaction-to-fire tests.

An in-depth study to verify this added mode of fire retardancy is presented here. In addition to the standard flammability measures discussed in ASTM E1354, this study also utilized imbedded thermocouples at various depths in the sandwiched panels and advanced evolved gas analysis to reveal the decomposition behavior of sandwich panels with and without an intumescent veneer coating. The construction of three sandwich panels with varying surface layers and the enhancement to the cone calorimeter gas analysis are described in the materials and methods section. In the results and analysis section, each relevant flammability feature is explained for the three sandwich panels for the exposure to irradiance at 50 kW m^{-2} and piloted ignition. Also from this dataset, the flame spread index classifications according to ASTM E84 [7] were estimated.

Materials and methods

Three variations for surface layers of foam core particle boards

Basically, the foam core particleboards with a nominal thickness of 19 mm were manufactured from a three-layered mat without additional gluing between the face and core layers. The resinated wood particles and urea formaldehyde resin (Kaurit 350, BASF, Germany) were used for the face layers. The expandable polystyrene (EPS, Terrapor 4, Sunpor, Austria) with a granule size of 0.3–0.8 mm was used as the core materials. According to the data sheet of Terrapor 4, it contains a small amount of flame retardant. It has been reported that fire retardants in foams work for very low ignition flux (<25 kW m^{-2}) but fire performance is essentially unchanged when larger ignition sources are used [8]. This material also contains 5.7 % pentane (by mass) as the blowing agent. An unpublished study has shown that between 2 and 3 % of the initial pentane remains in the foam cells after expansion, depending on process parameters (press temperature etc.).

The three-layered mat was then pressed in a lab-scale single opening (Siempelkamp, Germany) hot-press. The press cycle consist of three consecutive stages: pressing phase, foaming phase, and stabilization phase by the internal cooling of the press plates. The temperature of the press plates was set at 130 °C. The target overall density was 320 kg m^{-3} with a face density of 750 kg m^{-3} and a core density of 124 kg m^{-3}. Nominal surface thickness was 3 mm which corresponds to the foam core thickness of 13 mm and overall thickness of 19 mm. The pressing schedules and foaming conditions have been described in detail [1].

The two improvements utilized for this study were the use of conventional beech veneer without and with intumescent paper underneath the veneer. The fire resistive adhesive used for veneering the samples was Firobond Ultra Adhesive (FUA) supplied from ENVIROGRAF, UK. The sandwich panels without any veneer were utilized as reference samples in this series of tests. At least two panels of each series were produced as replicates and one sample was cut out from each panel to do the fire performance test. All the samples were conditioned at 23 °C and 50 % relative humidity for at least 2 weeks prior to testing to meet equilibrium moisture content (EMC).

Cone calorimeter upgrades and test procedure

The tests were carried out according to the ASTM E1354 test method with a cone calorimeter apparatus (Atlas Electrical Devices, Chicago, IL) at the Forest Product Laboratory in Madison, WI, USA. Samples were exposed

in the horizontal orientation to the irradiance of 50 kWm^{-2} after opening the water-cooled thermal shutter and the electric spark was used for piloted ignition. Prior to placing the specimen in the sample holder, four thermocouples were attached in the following manner. The exposed surface thermocouple (36 gauge Type K wire) was inserted into a slanted surface crevice formed with a razor blade. Two thermocouples (30 gauge Type K wire) were inserted in tiny long holes at the interface of the foam and particle board, with the bead situated at the sample's middle. The fourth thermocouple was taped to the backside surface at the sample's middle. These thermocouple measurements provided data to verify the insulating enhancements of the veneers. The Fig. 1 shows the position of the inserted thermocouples in the cross section of the samples.

The specimens were tested in the optional retainer frame with a wire grid over the test specimen. As explained earlier, some of the pentane remained in the specimen. After ignition of the surface layer, the elevated temperature eventually reaches the foam core layer. This temperature stimulates the remaining pentane in the foam to cause slight expansion of the foam during the test. To overcome excessive spalling and foam expansion that results in direct contact with the cone heater, a surface wire grid was used in all the cone tests to restrain the heated surface. Ignitability was determined by observing the time for sustained ignition of the specimen with a 4 s criteria for sustained ignition.

Exhaust gas composition was determined using three gas analyzers from Sable Systems (www.sablesys.com) and a relative humidity sensor from U.P.S.I. (www.upsi.fr). Oxygen was measured using the PA-10, a paramagnetic analyzer capable of resolution to 0.0001 % O_2 and modified to provide even faster response by reducing the internal volume of the filters. Exhaust gas to the sensor was dried using the Sable ND-2, a permeable-membrane dryer. Carbon dioxide was measured using the CA-10, a dual wavelength infra-red sensor capable of resolution to 1 ppm. The same technology was used in the CM-10A for carbon monoxide detection. Gas was delivered to the analyzers using two pumps. The first larger pump pulls exhaust quickly to the location of the Sable equipment through a pre-filter and water-bath controlled (50 °C) water-to-air heat exchanger to provide consistent incoming air conditions. Then, a sub-sample pumps pulls exhaust smoothly through the dryer and analyzers.

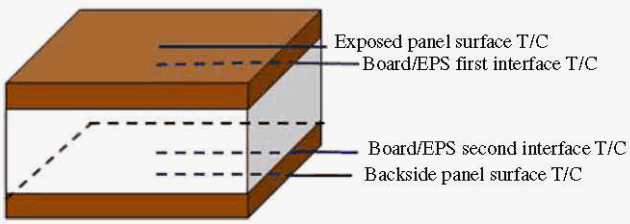

Fig. 1 The position of the thermocouples inserted in different places of the samples

The relative humidity was measured using the F-TUTA.34R, a quick responding sensor placed very early in the gas sample path inside the cone calorimeter. The lines and sample location were heated with heat tape to near 50 °C to avoid condensation on the lines after the ring sampler. The F-TUTA.34R provides analog signals corresponding to relative humidity and temperature. Similarly, the Sable components provide analog signals including the barometric pressure. These signals along with the type K thermocouple readings at various locations in the specimen were captured by the data acquisition system (Measurement Computing USB-1616HS) at 4 Hz. Raw signals were then time-shifted based on time-of-flight to the sensor to have all changes correspond to the mass loss signal from the cone calorimeter.

Exhaust flow rate calculations were based on Bernoulli's formula using pressure drop across the orifice, temperature of the exhaust, and various gas concentrations. Further fine tuning of the exhaust flow rate is based on matching the computed mass flow rates of depleted oxygen, carbon dioxide, and water with that determined from nearly complete combustion of pure ethylene glycol, fuel mass flow of which is measured with the weigh scale. As a basis for comparison, it has been found that for any incomplete hot combustion, the dynamic mass flow rate (g s^{-1}) of a fuel mixture with empirical formula $C_XH_YO_ZN_US_V$ has six equivalent calculations as derived from simple mass balances as [9],

$$
\begin{aligned}
\dot{m}_{\text{fuel}} &= \left(\frac{12X+Y+16Z+14U+38V}{32(X+V)+8Y-16Z}\right) \\
&\times \left(\Delta\dot{m}_{O_2}+\frac{32\dot{m}_s}{12}+\frac{16\dot{m}_{CO}}{28}+\frac{(32+8W)\dot{m}_{CHw}}{12+W}\right) > \text{Form 1} \\
&= \left(\frac{12X+Y+16Z+14U+38V}{44X}\right) \\
&\times \left(\dot{m}_{CO_2}+\frac{44\dot{m}_s}{12}+\frac{44\dot{m}_{CO}}{28}+\frac{44\dot{m}_{CHw}}{12+W}\right) > \text{Form 2} \\
&= \frac{12X+Y+16Z+14U+38V}{9Y}\left(\Delta\dot{m}_{H_2O}+\frac{9W\dot{m}_{CHw}}{12+W}\right) \\
&> \text{Form 3} = \frac{12X+Y+16Z+14U+38V}{14U}\Delta\dot{m}_{N_2} \\
&= \frac{12X+Y+16Z+14U+38V}{70V}\dot{m}_{SO_2} > \text{Forms 4 5} \\
&= \dot{m}_{CO_2}+\dot{m}_s+\dot{m}_{CO}+\Delta\dot{m}_{H_2O}+\dot{m}_{CHw}+\Delta\dot{m}_{N_2} \\
&+ \dot{m}_{SO_2}-\Delta\dot{m}_{O_2} > \text{Form 6}
\end{aligned}
\tag{1}
$$

with $X = 2$, $Y = 6$, and $Z = 2$ for ethylene glycol that is combusting completely, it is possible to use Forms 1, 2, 3,

and 6 to compare with the time derivative of the dynamic mass loss. No fine tuning of zero and span parameters for oxygen, carbon dioxide, and carbon monoxide gas analysis was needed, whereas the relative humidity sensor required minor calibration adjustments. To match up their response times from 10 to 90 % levels during step changes, small digital filtering was applied to sensor data for carbon dioxide, carbon monoxide, and water vapor, and a small digital deconvolution was applied to the oxygen sensor data. Since the molar fractions of O_2, CO_2, CO, and H_2O are now available and synchronized, the ASTM E1354 Annex procedure was utilized for calculating the mass flow rates, respectively, of the same molecules. The soot mass flow rate is merely calculated as the smoke production rate (product of volumetric rate and extinction coefficient) divided by the specific extinction area, 8.3 m^2 g^{-1}, for the black smoke. Estimates of *THCs*, although quite small, could reasonably have $w = 2$ in Eq. 1 and their mass flow rates ~0.1 % of the carbon dioxide mass flow rates corresponding to flaming combustion [10]. These mass flow rates are then substituted into Eq. 1 and some of the different forms of Eq. 1 are compared in Fig. 2 showing excellent agreement for burning of glycol. The calibrations derived for glycol burning was also applied successfully to the follow-on tests of the six sandwich panels for this study.

From Eq. 1 it can be derived, the further properties of the fuel combusted. Consider a volatile composition of fuel (tar), water vapor and carbon dioxide, $C_{X'}H_{Y'}O_{Z'}N_US_V + mH_2O + nCO_2$. The ratio of molar carbon content of the fuel mixture to its stoichiometric molar consumption of oxygen gas is derived as,

$$r_c = \frac{X' + n}{V + X' + Y'/4 - Z'/2} \cong \frac{\frac{\beta_{CO_2}}{44} + \frac{\beta_s}{12} + \frac{\beta_{CO}}{28} + \frac{\beta_{CHw}}{12+W}}{\frac{\beta_{O_2}}{32} + \frac{\beta_s}{12} + \frac{1}{2}\frac{\beta_{CO}}{28} + \frac{(1+W/4)\beta_{CHw}}{12+W}} \equiv \frac{8\beta_{CO_2,st}}{11} \tag{2}$$

Betas are merely the mass ratio of combustion product changes to oxygen depletion mass. We note that carbon fuel loading (Eq. 2) is independent of water content in any form because parameter m is factored out of Eq. 2. Carbon fuel loadings calculated for hydrogen gas, methane, propane, polystyrene, carbohydrates, carbon monoxide, carbon dioxide from Eq. 2, are respectively 0, 1/2, 3/5, 4/5, 1, 2, and 4 regardless of the H_2O content. Therefore, the use of carbon fuel loading can assist in identifying fuel, even when combustion becomes incomplete. Suppose that during a test period, the measured water vapor, excess nitrogen gas, sulfur dioxide, and *THC's* are attributed to material pyrolysis. Using Eqs. 1 and 2, further fuel properties are derived as,

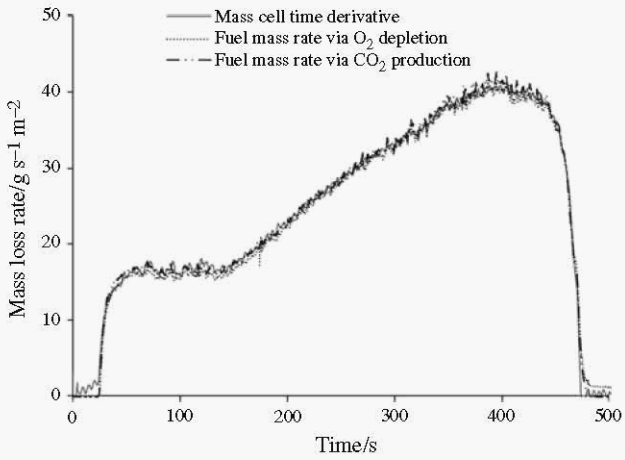

Fig. 2 Comparison of fuel mass rate between gas analysis and mass cell time derivative

$$\frac{Y}{X} = \frac{Y' + 2m}{X' + n} = \frac{[\dot{m}_{H_2O}/9 + W\dot{m}_{CHw}/(12 + W)]}{\frac{\dot{m}_{CO_2}}{44} + \frac{\dot{m}_s}{12} + \frac{\dot{m}_{CO}}{28} + \frac{\dot{m}_{CHw}}{12+W}} \cong \frac{[\beta_{H_2O}/9 + W\beta_{CHw}/(12 + W)]}{\frac{\beta_{CO_2}}{44} + \frac{\beta_s}{12} + \frac{\beta_{CO}}{28} + \frac{\beta_{CHw}}{12+W}} \tag{3}$$

$$\frac{Z}{X} = \frac{Z' + m + 2n}{X' + n} = 2 + \frac{2V}{X} + \frac{Y}{2X} - \frac{11}{4\beta_{CO_2,st}} \tag{4}$$

For wood, the stoichiometric net heat of combustion (kJ g^{-1}) is correlated closely as [11],

$$h_{c,st} = 13.23 r_o \tag{5}$$

$$r_o = (32X + 8Y - 16Z)/(12X + Y + 16Z + 14U + 38V) \tag{6}$$

Polystyrene, C_8H_8, (r_o = 3.077), has the value 12.93 instead of 13.23 in Eq. 5. Indeed, carbon solid and carbon monoxide fuel has further deviations, such that the heat release due to incomplete combustion (producing C and CO from oxidizing the organic carbon) has the adjustment to Eq. 5 as [11],

$$\text{HRR} = 13.23\Delta\dot{m}_{O_2} - 2.54\dot{m}_{CO} + 2.48\dot{m}_s \tag{7}$$

The holocellulose, as the major component, is made up mostly alpha cellulose, mannan, and galactan that has the empirical formula, $C_6H_{10}O_5$, (r_o = 1.185), while minor components are xylan and arabinan with a slightly different empirical formula. Its heat of combustion via Eq. 5 is in agreement with the measured value for fully volatized holocellulose [11]. An empirical formula of lignin can be used as $C_9H_6O_2(H_2O)(OCH_3)_{4/3}$, ($r_o$ = 1.74), which also has net heat of combustion via Eq. 5 in agreement with that measured for fully volatized lignin [11]. In the case of extractives, monoterpenes is the main component with empirical formula, $C_{10}H_{16}$, (r_o = 3.294), which is consistent via Eq. 5 for the net heat of combustion [11].

This also predicts that Eq. 6 is linearly related to mass fractions of extractives, holocellulose, and lignin for any wood material and was established to a high correlation [11]. If any of the constituents are also charring, then its corresponding volatiles have a differing empirical composition than that of the virgin material, due to retaining the carbon into the char. As a result, the net heat of combustion of wood volatiles is not straightforward, requiring the techniques offered by the use of Eqs. 1–6. Therefore, for all samples, the composition ratios of $r_c, Y/X$, Z/X, and r_o as a function of time will be discussed in the context of improving flammability performances with fire retardancy.

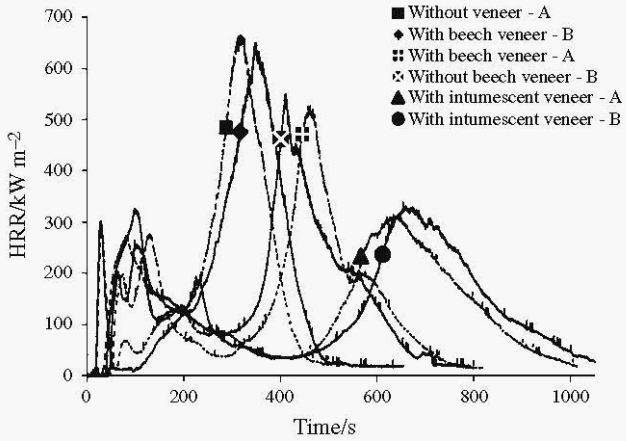

Fig. 3 Comparing sandwich panel HRR with three surface layer constructions

Results and discussion

Heat release rate (HRR) of panels with three surface layer variations

The potential fire hazard of a combustible material can be indicated by the heat release rates (HRR). Figure 3 shows the HRR profile, as computed with Eq. 7, having the dual peak HRR profiles. The first peak is the result of ablating initially the surface exposed to a combined cone heater and flame radiance on the surface. The HRR then decreases as a result of surface charring and the thermal wave process following the ablative process. In essence, the pyrolysis front develops and is decreasing in speed, and with the char density staying constant, the volatilization mass rate is also decreasing. Since the volatile heat of combustion is fairly constant for initially dry wood (as shown later in Figs. 6, 9, and 12 during dry portions of particle board volatilization), the HRR is also decreasing [11, 12]. The HRR eventually begins to rise as a result of the thermal wave termination at the insulated rear surface, which means the sample is entering the thermally thin regime, and broadens and speeds up the thin pyrolysis zones. For a surface layer sufficiently thin and backed by an insulation board such as EPS, the dual peaks in the HRR merge together into a single initial peak, such that the surface is treated as thermal capacitance that controls the heating process, and thus the pyrolysis process [9]. However, since there is a second, backside surface layer of particle board, it is just a matter of time after the EPS has fully melted and charred remains of the exposed surface layer heats the backside surface layer by contact or radiation. Further volatilization occurs when the backside particle board reaches its volatilization temperatures after a period of heating. The glowing from the infusion of air takes over at some point, and as the material is consumed the HRR will decrease once again. More detailed measurements developed for this study is presented in later sections to explain further this pyrolysis process.

Indeed, the size of a fire is correlated positively with the HRR and the HRR will in turn increase as the fire is spreading, unless the HRR can be made to decrease rapidly enough (burnout) or be kept to a low value to counter the increase in pyrolysis surface area effects on the HRR [13]. That is, fire retardancy would serve its purpose by preventing fire growth (i.e., resulting in low HRR values) rather than merely preventing ignition. The other factor is that the ASTM E84 flame spread test lasts 10 min, so that only the first 600 s of the cone calorimeter test is relevant for this regulatory test. In addition, the ASTM E84 specimen is backed by a heavy cement board that will absorb heat from the exposed specimen (the thermal wave moves on through rather than terminating), thereby drastically reducing the second HRR peak [13] and extending the period of glowing. However, there are real world fires in which the insulation backing is more the norm, which suggests alternate flame spread testing might be more appropriate to evaluate fire retardancy at full scale for these cases.

It is seen that some reduction of the HRR profile in Fig. 3 is obtained with the beech veneer adhered with Firobond Ultra Adhesive by EnviroGraph (FUA) to both sides of the sandwich panel, whereas the second large peak HRR peaking at 450 s is both decreased and delayed and some HRRs are now observed beyond 600 s. However, the use of the veneer with intumescent paper (ES/MP/DK by Intumescent Systems LTD) adhered with FUA to both sides of the sandwich panel, has decreased HRR overall and the majority of the HRRs are now greater than 600 s. The repeated tests confirmed this result. The HRR profiles that are most amenable to analytical fire growth modeling are that of exponential decay function, for predicting the flame spread rating for the ASTM E84 test method that was successful with oriented strand boards (OSB), treated and untreated. Since the second large HRR peak can be ignored because of the heavy backing board, the closer attention to

the first peak is targeted for this exponential decay function approximation. Wood products with peak HRR around 300 kW m^{-2} are known as Class C materials [13] according to ASTM E84 test method. If the initial narrow peak HRR for the intumescent veneered panel is also ignored in Fig. 3, then a fitted exponential decay has the PHRR lowered to 100 kW m^{-2}, ignition time increased to 55 s (using a high density veneer), and the total heat release (THR) remaining at 117 MJ m^{-2}, should predict a Flame Spread Index in Class A category [13]. Further investigations with targeted variations of the surface layer should have merit.

Pyrolysis mechanisms of panels with three surface layer variations

The thermal conductivity of the EPS foam strongly affects the fire performances. Due to its low thermal conductivity, in the range 0.03–0.04 W mK^{-1}, expanded polystyrene foam acts as a protective layer underneath of the woody surface layer with its thermal conductivity of around 0.13 W mK^{-1}. This leads to an intensive heating of the surface layer [5]. Accordingly, an increased first peak of heat release rate significantly higher than that of conventional particleboard does occur. After surface ignition (and prior to the point of PHRR at 30 kW m^{-2}) char formation starts, and the volatile emission rate is affected by the speed of the pyrolysis front propagating into the wood-based material. While the surface layer is burning the foam core layer first melts and then starts volatizing. The foam does not char and its volatiles with their corresponding higher heat of combustion begin to be added to that of the wood volatiles. This can be detected also with thermocouples by which polystyrene decomposition is indicated when temperatures around 350 °C are reached. At this time, the pyrolysis zone reaches the back face of the samples and causes the so-called thermal feedback effect [3]. The second Peak HRR is due to the volatizing of the foam and the back surface layer, and also to a transition to glowing, which is seen by heat of combustion approaching 30 kJ g^{-1} or r_o reaching 2.67 to correspond with pure carbon (i.e., the char becomes mostly carbon, but will not combust until the air is able to penetrate after the volatiles has ceased emitting). Because of the challenge posed by the presence of the EPS foam core, a fundamental study was made of panel with three layer variations as reported here.

Mass loss rate, temperature profile, and volatile features of panel without veneer

For the sandwich panel without veneer, it is seen that fuel mass rate derived from the gas analysis using Eq. 1 is in agreement with the mass cell time derivative for combustion times after ignition in Fig. 4. This figure shows the dual peak feature noted for the corresponding HRR profiles. The temperature profiles in Fig. 5 demonstrate the insulation capabilities of the exterior board only lasted for 100 s before the EPS settled at the highly degrading temperatures around 500 °C until glowing began. The composition features shown in Fig. 6 make apparent that significant water evaporation (high *Y/X* and *Z/X* ratios) occurs at the beginning and at 150 s. Thus during the time up to 150 s, the free moisture moved to the back side under temperature gradient, and when the heat became available after the collapse of the EPS foam, the accumulated moisture evaporated in large amounts and was able to dilute the volatiles to cause a temporary reduction in r_o (also net heat of combustion) values. The carbon loading remains close to unity, verifying that the volatiles and

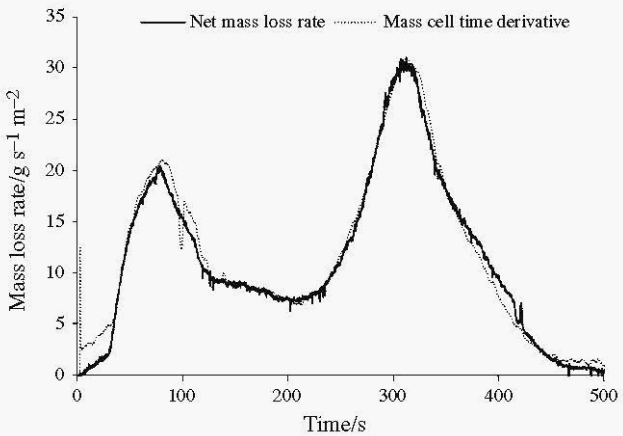

Fig. 4 Using Form 6 of Eq. 1 to calculate fuel mass rate in agreement with mass cell time derivative for un-veneered samples

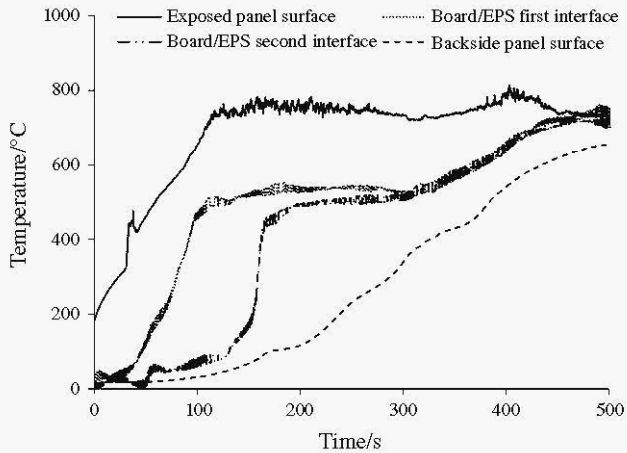

Fig. 5 Temperature measurements at various depths for un-veneered samples

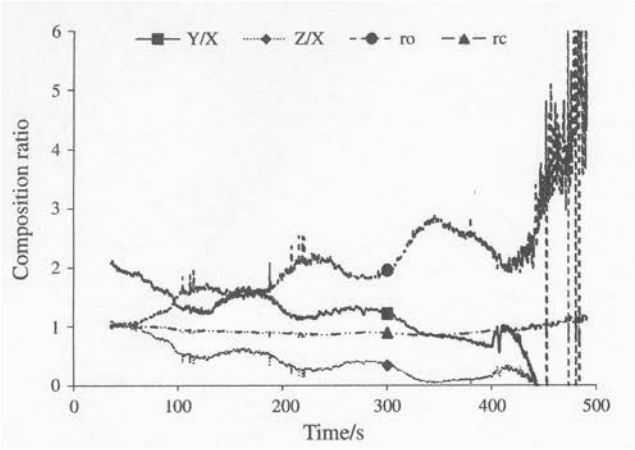

Fig. 6 Derived empirical compositions of pyrolysis for un-veneered samples

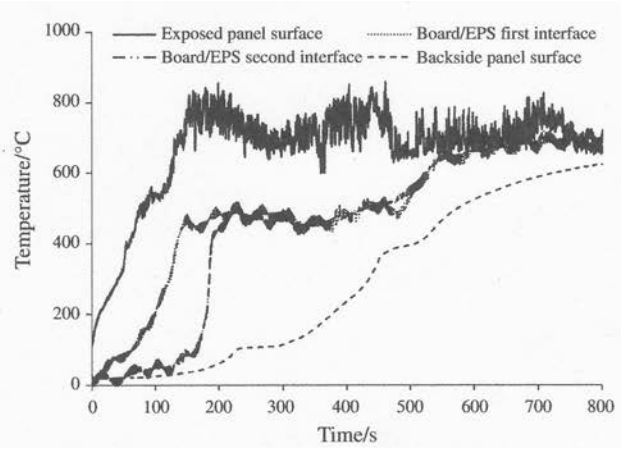

Fig. 8 Temperature measurements at various depths in the panel with beech veneer

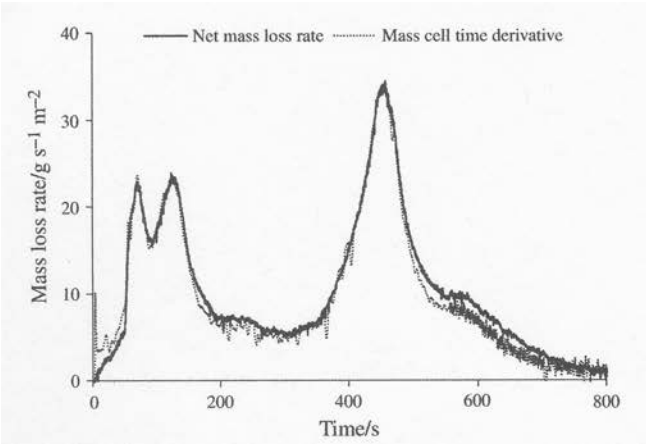

Fig. 7 Using Eq. 1 to calculate fuel mass rate in agreement with mass cell time derivative for panel with beech veneer

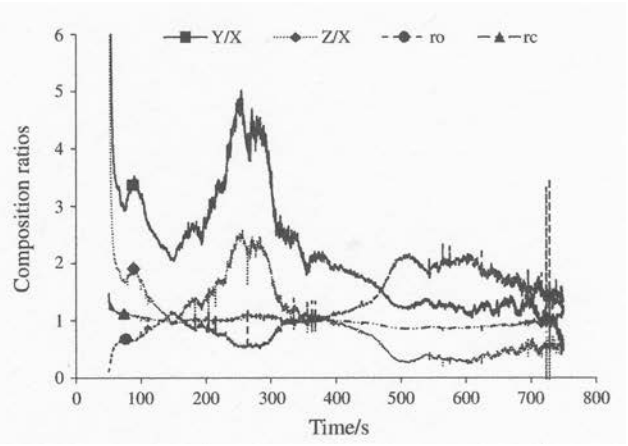

Fig. 9 Derived empirical compositions of pyrolysis for panel with beech veneer

glowing char have carbohydrate-type empirical form. Finally, the ratio *Z/X* goes to zero and *Y/X* goes to unity while r_o values are reaching 2 or beyond at the time 325 s that indicates glowing combustion of highly carbonized char.

Mass loss rate, temperature profile, and volatile features of panel with beech veneer

For the sandwich panel with the beech veneer, we likewise get good predictions of the fuel mass rate with the gas analysis, and Fig. 7 shows a triple peak feature as also seen in the corresponding HRR profile. It is seen that nearly all pyrolysis still occurred within 600 s corresponding to ASTM E84 test time. Temperature profiles in Fig. 8 still show the EPS degrading at temperatures around 450 °C beginning at time 150 s. The empirical composition of the volatiles at 150 s in Fig. 9 possibly shows the presence of EPS volatiles (carbon loading less than one and r_o peaking), while the evaporation of water that has piled up toward the backside occurred at 250 s (quite high values of *Y/X* and *Z/X*), and finally the glowing combustion sets in at the time 500 s (*Y/X* approaching one, *Z/X* approaching zero, carbon loading slightly less than one, and r_o approaching 2 and higher). However, this is not much improvement in flammability properties.

Mass loss rate, ,temperature profile, and volatile features of panel with intumescent veneer

For the sandwich panel with intumescent veneer paper, once again good agreement of the fuel mass rate from gas analysis with the load cell time derivative is obtained in Fig. 10, and it is seen that more of the pyrolysis is occurring after 600 s, thereby effectively reducing the HRR contributing to the ASTM E84 test environment. The temperature profiles shown in Fig. 11 show that EPS remained below the degradation temperature of 350 °C at

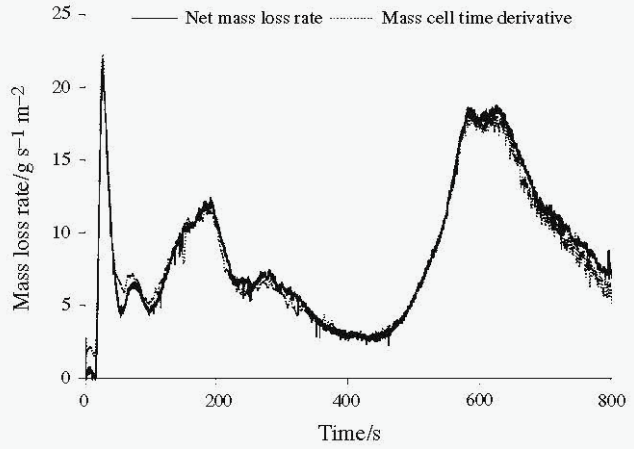

Fig. 10 Using Eq. 1 to calculate fuel mass rate in agreement with mass cell time derivative for panel with intumescent veneer

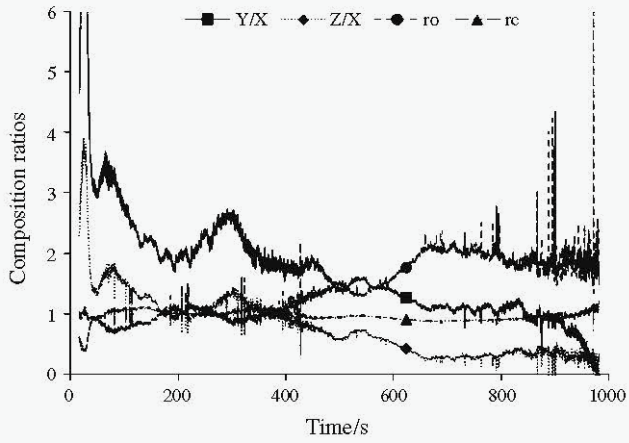

Fig. 12 Derived empirical compositions of pyrolysis for panel with intumescent veneer

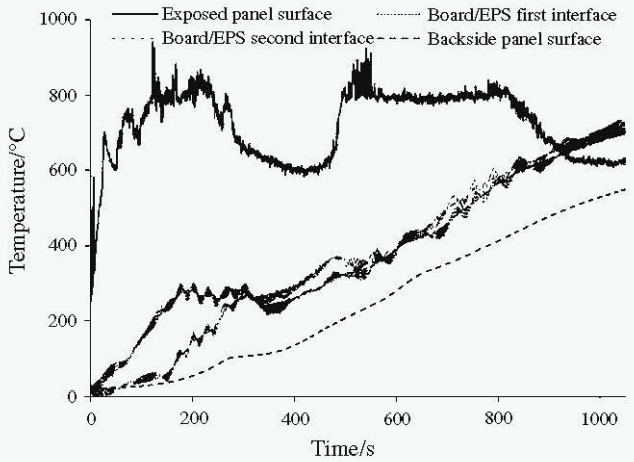

Fig. 11 Temperature measurements at various depths of the panel with intumescent veneer

times up to 600 s. In the empirical composition plots shown in Fig. 12, it is apparent that glowing began around 500 s. It is seen from the high values of *Y/X* and *Z/X* at ratios of four and two respectively showed the moisture contribution from the intumescent paper up to 200 s. At 300 s another incident of water evaporation is present from the moisture driven to the panel backside via temperature gradients. At times surrounding 200 and 400 s, the *Y/X* is about 2, and *Z/X*, r_o and r_c are around 1, all of which are closely the features of wood pyrolysis without water vapor and EPS volatiles.

Conclusions

In order to assess the fire retardant properties of novel sandwich panels, advanced cone calorimetry techniques were devised. Four thermocouples attached to the specimen at the various depths were used to determine the physical state of the EPS foam core that defined softening, melting, decomposition, and ignition. A state-of-art gas analysis procedure was devised to determine composition features of panel pyrolysis, which resulted in validating the calculations of empirical composition of the volatiles as *Y/X* and *Z/X*, and of carbon loading and oxygen mass to fuel mass ratio. HRR of sandwich panels having surface layers with either beech veneer or intumescent veneer paper is lowered and delayed in comparison to those without veneer, and significantly so for panels with the intumescent veneer paper. Results for cone calorimeter tests at 50 kW m^{-2} show that the intumescent veneer paper composite protected the core EPS foam from degrading, as well as seal and dilute wood volatiles in the early stages of pyrolysis, to where it may be possible to achieve a Class A flame spread rating. Although the measured O_2, CO_2, CO, H_2O and soot mass flow rates were used in the determination of the pyrolysis properties, they were not presented directly in this paper, as they are suited to the study of combustion emissions, in contrast to the fundamental study of material pyrolysis and their effect on the HRR profiles for this work.

Acknowledgements The authors wish to thank Dr. Robert White and Carol Clausen of the Forest Products Laboratory for their support of this research, and to technician Ms. Anne Fuller for collecting the data. We also thank Hamburg University and Ministry of Science, Research & Technology of Iran for financial support of this work and of Dr. Luedtke for support of this research. The work was performed by the United States employees on official time and is not subject to copyright.

References

1. Shalbafan A, Luedtke J, Welling J, Thoemen H. Comparison of foam core materials in innovative lightweight wood-based panels. Holz Roh Werkst. 2012;70:287–92.

2. White RH, Dietenberger MA. Cone calorimeter evaluation of wood products. In: Proc. 15th Annual BCC Conference Flame Retardancy. USA Stanford, Connecticut; 2004.
3. Schartel B, Bartholmai M, Knoll U. Some comments on the use of cone calorimeter data. Polym Degrad Stabil. 2005;88:540–7.
4. ASTM E 1354-11a. Standard test method for heat and visible smoke release rates for materials and products using an oxygen consumption calorimeter. West Conshohocken: ASTM International: 2011.
5. Shalbafan A, Dietenberger MA, Welling J. Fire performances of foam core sandwich panels continuously produced in different pressing schemes. Holz Roh Werkst. 2012:. doi:10.1007/s00107-012-0653-4.
6. Gurman JL, Baier L, Levin BC. Polystyrenes: a review of the literature on the products of thermal decomposition and toxicity. Fire Mater. 1987;11:109–30.
7. ASTM E84-03. Standard test method for surface burning characteristics of building materials. West Conshohocken: ASTM International: 2011
8. Babrauskas V, Parker WJ. Ignitability measurements with the cone calorimeter. FireMater. 1987;11:31-43.
9. Dietenberger MA. Pyrolysis kinetics and combustion of thin wood by an advanced cone calorimetry test method. J Therm Anal Calorim. 2012:. doi:10.1007/s10973-0122474-4.
10. Barrefors G, Petersson G. Volatile hydrocarbons from domestic woodburning. Chemosphere. 1995;30:1551–6.
11. Dietenberger MA. Update for combustion properties of wood components. Fire Mater. 2002;26:255–67.
12. White RH, Dietenberger MA. Chapter 18: Fire safety of wood construction. In: Ross RJ (ed) Wood handbook wood as an engineering material. Madison: Forest Products Laboratory, Department of Agriculture Forest Service: 2010.
13. Dietenberger M A White RH. Reaction-to-firetesting and modeling for wood products. In: Proc. 12th Annual BCC Conference on Flame Retardancy. USA: Stamford, Connecticut: 2001. p. 54–69.